Available online at www.sciencedirect.com
SCIENCE DIRECT®
Nuclear Instruments and Methods in Physics Research A 513 (2003) 107–111
NUCLEAR INSTRUMENTS & METHODS IN PHYSICS RESEARCH Section A
www.elsevier.com/locate/nima

The silicon Multiplicity Detector for the NA50 experiment

B. Alessandro[a], S. Beole[b], G. Bonazzola[b], W. Dabrowski[c], P. Deremigis[a], P. Giubellino[a], P. Grybos[c], M. Idzik[a,c,*], A. Marzari-Chiesa[b], M. Masera[b], M. Monteno[a], W.L. Prado da Silva[d], F. Prino[e], L. Ramello[e], P. Rato Mendes[b], L. Riccati[a], M. Sitta[e]

[a] *INFN, Torino, via P. Giuria 1, Torino 10125, Italy*
[b] *Dipartimento di Fisica Sperimentale dell'Universita, Torino, Italy*
[c] *Faculty of Physics and Nuclear Techniques, University of Mining and Metallurgy, Cracow, Poland*
[d] *UERJ, Rio de Janeiro, Brazil*
[e] *DISTA, Universita del Piemonte Orientale, Alessandria, Italy*

Abstract

The operation and performance of the silicon strip Multiplicity Detector in the heavy-ion experiment NA50 at CERN are presented together with a selection of physics results. The main features of the detector are high speed (50 MHz sampling frequency), high granularity (more than 13,000 strips), and good radiation resistance. The detector provided a measurement of event centrality in Pb–Pb collisions, as well as target identification and the measurement of charged particle pseudorapidity distributions as a function of centrality.

PACS: 29.40

Keywords: Position sensitive detector; Silicon strip detector; Front-end electronics; Experimental techniques; Data analysis

1. Introduction

The NA50 experiment [1] at the CERN SPS investigates nuclear matter under extreme conditions of energy density with the ultimate goal of detecting signals of a phase transition from ordinary matter to a plasma of deconfined quarks and gluons (QGP). In particular the experiment is looking for dimuon production from charmonium resonances and its suppression due to Debye screening in a deconfined medium [2] in fixed-target Pb–Pb interactions at 158 A GeV/c beam momentum. To collect enough Journal logo statistics on the production of J/ψ and ψ' mesons, the experiment worked at the maximum beam intensity which was compatible with a correct operation of the various detectors, namely $(1–1.4)\times 10^7$ beam particles/s, and with a target thickness up to 32% of an interaction length. The main detector components are a high resolution muon spectrometer and three centrality detectors, namely a zero-degree calorimeter (ZDC) for forward energy (E_{ZDC}) measurements,

*Corresponding author. Address for correspondence: INFN, Torino, via P. Giuria 1, Torino 10125, Italy. Tel.: +39-011-670-7372; fax: +39-011-669-9579.
E-mail address: idzik@to.infn.it (M. Idzik).

0168-9002/$ - see front matter © 2003 Elsevier B.V. All rights reserved.
doi:10.1016/j.nima.2003.08.012

an electromagnetic calorimeter (EMC) for transverse energy (E_T) measurements and a silicon microstrip Multiplicity Detector (MD) for charged particle multiplicity measurements [3]. The MD was also used to identify whether the interaction took place in the target.

A very fast binary readout electronics scheme was chosen to provide the excellent double pulse resolution required by the high beam rate. It consists of an analog and a digital chip. The former (FABRIC) [4] includes preamplifier ($T_{peak} = 15$ ns), shaper and discriminator, while the latter (CDP) [5] is a digital buffer working with sampling frequency of 50 MHz. The need to suppress the background due to the decays of π and K mesons imposed an absorber very close to the target, and therefore a very small space available for the silicon detectors. Two discs (MD1, MD2) of radial silicon microstrip detectors, 10 cm apart, were built. The inner radius of the detectors in each disc is 0.5 cm while the outer one is 8.5 cm. The detector granularity was mainly determined by particle occupancy, keeping it below 30%. Taking into account also multiple scattering in the target and size of the beam (0.5 mm RMS) a constant segmentation of the detector $\Delta\eta = 0.02$ in pseudorapidity and $\Delta\phi = 10^0$ in azimuth angle was chosen. So each disc consists of 36 azimuthally segmented sectors, 192 strips in each sector. Estimated fluences and doses for the innermost part of the detector were, respectively, 10^{14} particle/cm^2 and 10 Mrad, while for the front-end electronics region 10^{12} particle/cm^2 and 200 krad, respectively. Standard p–on–n detectors and a full-custom rad-hard front-end electronics were chosen. A single detector disc is shown in Fig. 1.

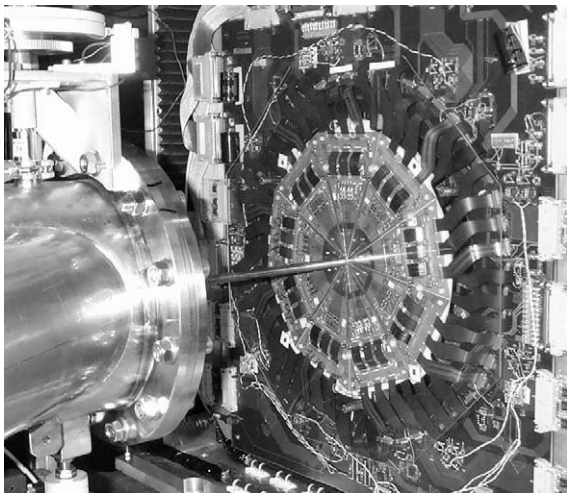

Fig. 1. Picture of MD1.

2. Setting up and operation

In order to establish the initial working conditions of the MD, and to maximize the detection efficiency, it was necessary to set and periodically verify some control parameters: the trigger delay, the threshold voltage of the FABRIC discriminators, and the biasing voltage of the silicon detectors [6]. In addition, an initial geometrical alignment on the beam line was made at the beginning of each data-taking period, which later on, was refined using experimental data. Some of these controls are discussed in this section.

2.1. Trigger delay

The trigger latency period was about 1 μs, while the time interval necessary to have the CDP pointer on the RAM column where the triggered event was stored was 1.6 μs, corresponding to 80 clock cycles of 20 ns duration (at 50 MHz frequency). So it was necessary both to align the phase of the trigger signal with the CDP clock, and to add the right amount of delay. The optimization of the delay value was done during a series of short acquisition runs (trigger delay scan). Fig. 2 shows the results of such a scan for a typical detector, both for low beam intensity (about 10^6 Pb/s) with minimum bias (ZDC) trigger, and for high beam intensity (about 10^7 Pb/s) with dimuon trigger. The peak occupancy with low intensity beam and ZDC trigger corresponds essentially to non-interacting Pb ions giving δ-rays plus a small fraction of Pb–Pb interactions. The peak occupancy for dimuon trigger is of course higher, since it corresponds to the inelastic Pb–Pb interactions, and is found for the same delay value as for the ZDC trigger. Since the actual sampling instant of the FABRIC

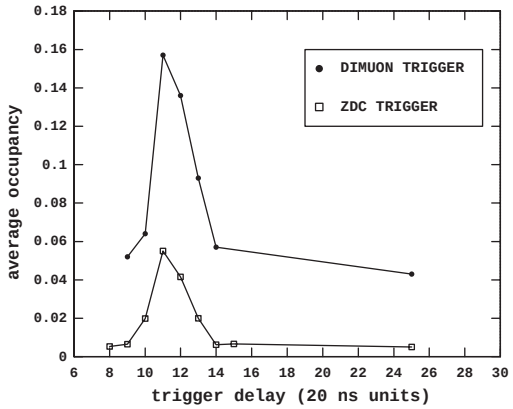

Fig. 2. Average occupancy per strip vs. trigger delay.

discriminator output must be in phase with the free-running CDP clock, the sampling efficiency may depend on the time difference between sampling and trigger (the latter is strictly related to particles crossing the detector). This difference was recorded by a TDC installed specially for this purpose. Usually there was a wide efficiency plateau and only a small TDC-based offline correction was necessary when evaluating the total multiplicity.

2.2. The discriminator threshold voltage

In order to set the correct discriminator threshold for the analog chip and to measure the signal to noise ratio (S/N) of our system, a few threshold scans with the SPS proton beam impinging directly on the detector were made. Fig. 3 shows the not normalized integral occupancy curve and its derivative. In order to estimate the MIP peak position a simple gaussian fit is performed only in the region around the peak of the differential curve. From these curves we estimate the MIP peak to be at about 470 mV. The gaussian noise evaluation from a separate study with pulser gave $\sigma_{\text{noise}} = 30$ mV, what would result in a S/N ratio of about 15. In fact during standard Pb–Pb runs operation of the whole system we observed higher rate of noise counts than expected from the measured σ_{noise}. This could be attributed to pick-up from the digital part of the front-end electronics. One should remember that a binary system

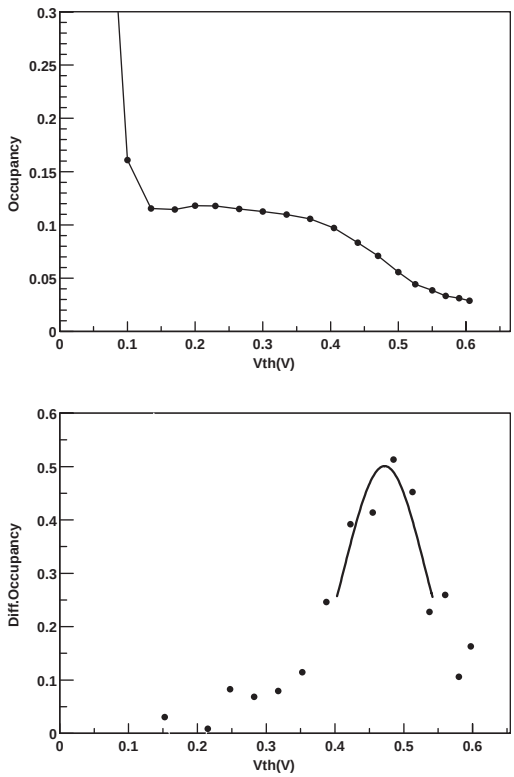

Fig. 3. Occupancy per strip vs. threshold voltage with proton beam (top: integral curve, bottom: differential curve).

working at a strip occupancy of about 10–30% has a very high rate of switching between high and low voltage states, which could give rise to some non-gaussian noise component. Taking into account the system performance in standard conditions we fixed the FABRIC threshold at the relatively high level of about 200 mV. This value was adjusted several times during different years of operation separately for MD1 and MD2 detector planes.

Threshold scans taken with secondary particles produced in Pb–Pb interactions were recorded from time to time for this purpose.

2.3. The geometrical alignment

The position of each detector with respect to geometrical references in the supporting stesalite disc was measured with an accuracy of about 50 μm. These geometrical data were used in a simple geometrical Monte-Carlo program to

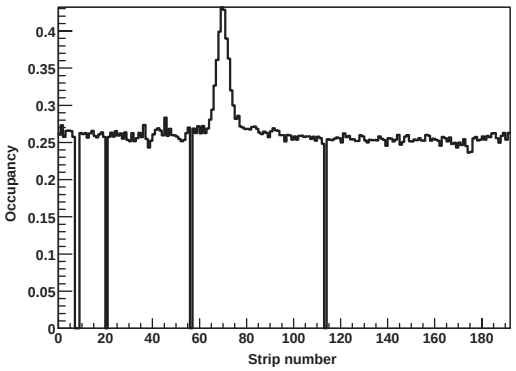

Fig. 4. Correlation between chosen strip of MD1 and corresponding sector of MD2.

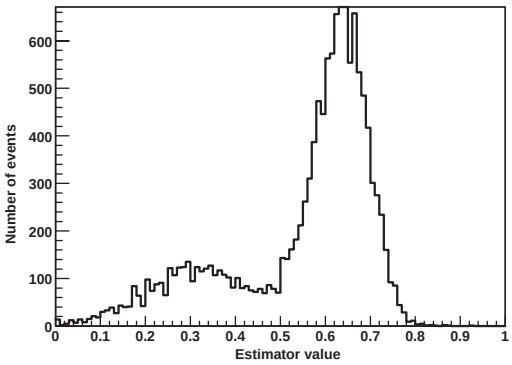

Fig. 5. Estimator distribution for target 4.

compute, for each target, the distribution of strips on MD2 corresponding to a given strip on MD1 for each sector. This was done under the assumption that the corresponding strips are defined from the position of MD1 and MD2 hits by a particle originating from a given target.

The MD1–MD2 strip correspondences were also obtained from the measured data where, for events with a particular MD1 strip being hit, a peak position and width in the MD2 occupancy map was found (see Fig. 4). The correspondences obtained from the geometrical Monte-Carlo were compared with the ones extracted from experimental data. The beam offsets in X and Y adopted in the Monte-Carlo were tuned until a good agreement with real data was obtained: the beam offsets found in this way were about 1 mm in Y and 0 mm in X, with a precision of about 0.2 mm.

3. Results

3.1. Target identification

An important result from the MD has been the identification of interactions coming from the target, which must be separated from those due to Pb–air interactions or upstream/downstream interactions. The identification is based on the comparison of estimators for different target positions, using the MD1–MD2 correlations discussed previously. The estimators were defined as the ratio of found MD1–MD2 strip correspondences to the number of possible correspondences, under different hypotheses on the interaction position (namely target, nearby surrounding air and target box windows). In Fig. 5 the estimator distribution for semi-central interactions is shown.

The peak at high estimator values identifies Pb–Pb interactions while the smaller peak at lower estimator values corresponds to other competitive processes like Pb–air interactions. Setting the appropriate threshold for the estimator value one can select only events coming from target interactions. The threshold value will depend somewhat on the event centrality since the number of random correspondences between multiplicity planes grows with particle occupancy. The study of estimator distributions in different centrality classes was done in order to set the right thresholds and to select minimum bias event samples for further analysis.

3.2. Centrality estimation

The MD provided the estimation of centrality via the global measurement of the charged multiplicity. As an example, the correlation between multiplicity (MUL1) and E_T is shown in Fig. 6.

3.3. Charged particle pseudorapidity distributions

The MD provided also detailed pseudorapidity distributions as a function of centrality, for two-beam energies [7]. Two analyses were performed using two independent centrality-related

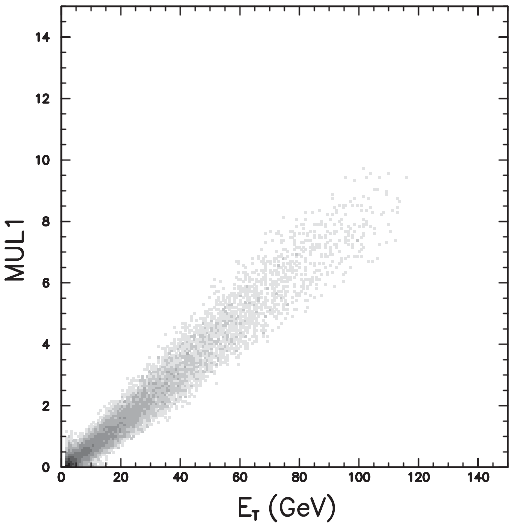

Fig. 6. Correlation between charged multiplicity and ET.

observables: the energy of the projectile spectator nucleons measured by the ZDC and the neutral transverse energy measured by the EMC. In both cases, the centrality selection was made using observables, which are independent of the MD itself, in order to avoid autocorrelations. Special runs taken with the minimum bias trigger at low beam intensity were used for the sample taken at 158 GeV/nucleon and the second at 40 GeV/nucleon energy. The charged particle pseudorapidity distributions $dN_{ch}/d\eta$ in Pb–Pb collisions were measured in six centrality classes defined in terms of fractions (between 0% and 35%) of the total inelastic cross-section.

4. Conclusions

We have operated and analyzed data from a silicon strip Multiplicity Detector (MD) in the challenging environment of the NA50 experiment. Very severe timing spatial and radiation constraints have been satisfied with a design based on standard p–on–n detectors and full-custom radiation-hard very fast front-end electronics. The MD has provided centrality measurement and target identification in Pb–Pb collisions for the NA50 data taken between the years 1995 and 2000. The charged particle pesudorapidity distributions as a function of centrality have also been measured.

Acknowledgements

We are grateful to the members of the NA50 collaboration who provided a stimulating and friendly working environment during the construction and operation of the detector. Financial support from the Istituto Nazionale di Fisica Nucleare of Italy is acknowledged. This work was supported in part by the Polish State Committee for Scientific Research, Project no. 2P03B03319.

References

[1] M.C. Abreu, et al., Study of muon pairs and vector mesons produced in high energy Pb–Pb interactions, Proposal CERN/SPSLC 91-05, SPSLC/P265, October 1991.
[2] T. Matsui, H. Satz, Phys. Lett. B 178 (1986) 416.
[3] B. Alessandro, et al., Nucl. Instr. and Meth. A 409 (1998) 167.
[4] W. Dabrowski, et al., Nucl. Instr. and Meth. A 350 (1994) 548.
[5] J. DeWitt, IEEE Nuclear Science Symposium, San Francisco, October–November 1993.
[6] B. Alessandro, et al., Nucl. Instr. and Meth. A 432 (1999) 342.
[7] M.C. Abreu, et al., Phys. Lett. B 530 (2002) 33.